Available online www.jsaer.com

***Journal of Scientific and Engineering Research*, 2019, 6(3):188-195**

Research Article

ISSN: 2394-2630
CODEN(USA): JSERBR

Experimental Study of Impingement Cooling of Flat Surface Utilizing Unconfined Chevron Jets

Missaid M. S. M. A. Almutairi[1,*], Hussein M. Maghrabie[2], M. Attalla[2], Mustafa Abd EL-Fatah[3]

[1]Ministry of Electrical and Water –Industrial El-Shuk Zone, Kuwait – Kuwait
[2]Department of Mechanical Engineering, Faculty of Engineering, South Valley University, Qena 83521, Egypt
The High Institute of Engineering and Technology, El-Tud, Luxor, Egypt
* Corresponding Author: Missaid M. S. M. A. Almutairi

Abstract Effect of chevron nozzle number on local and average Nusselt number over a flat plate impinged by air jets is studied. The Reynolds numbers of 8000, 7000, 6000, 4500, 3500, 2500, and 1400.Three different chevron nozzle configurations are studied (N= 0, 4, and 6) with a pipe diameter of 9 mm. Thin metal sheet technique is used with IR camera to measure the wall temperature at nozzles to separation distances (H/d = 2, 4, 6, and 8).

Keywords local Nusselt number, stagnation point, chevron, average Nuuselt number

1. Introduction

In the last two decades, the impinging jet technique has been become popular due to widespread cooling, heating and drying industrial application. The unique inherent characteristics of impinging jet are high local heat and mass transfer that is due to flow is directed to the target surface. The applications examples are cooling the gas turbine blades and vanes, drying papers and food products, cooling the electronic devices, quenching operation in glass industry. Also in laser or plasma cutting process, the impinging jet is used to cool down the products locally in order to avoid deformation. Figure 1 illustrates the simple schematic of round impinging jet on a target plate [1-9].

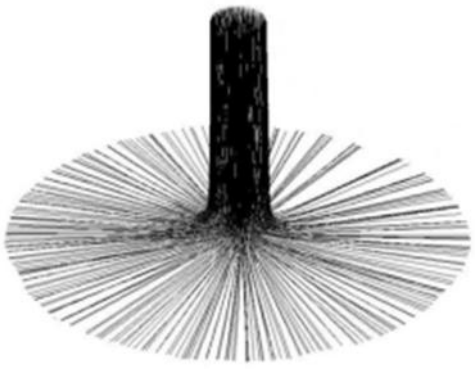

Figure 1: Schematic diagram of round jet flow on flat surface.

In the recent years, many attentions to the impinging jet has been paid by researchers not only because of effect of different parameters and interesting physic of impinging jet, but because of effort to validate turbulence models to predict impinging jet characteristic and complex pattern in different zones from free shear layer to

near wall boundary condition. Many analytical studies reported the hydrodynamics of the impinging jet that the jet consists of three separate different regions; the free jet region, the impingement region, and the wall jet region as illustrated in Figure 2 [3]. The characteristics of the free jet region where the flow is in a vertical direction, is not affected by the presence of the impingement space. The free jet region has two sub-regions.

- The potential core: In this region the flow velocity equals the jet exit velocity. The length of the potential core is the distance between the nozzle and the point where the centerline velocity begins to decrease.
- The lower-velocity mixing layer: There is the flow region beyond the potential core. The velocity profile in this region is well developed and the free jet centerline velocity decays.

In the impingement region, the flow is decelerated in the axial direction and accelerated in the radial direction. The stagnation region has the higher heat transfer characteristics than other region due to the higher shear stress [3, 10-16]. While in the wall jet region, the flow spreads out radially over the surface. The pressure distribution in this region is essentially equals to the ambient pressure [14]. The most important parameters that affect the hydrodynamic of the jet are: the distance between component and the orifice plane, the orifice diameter, orifice length, and the jet velocity are.

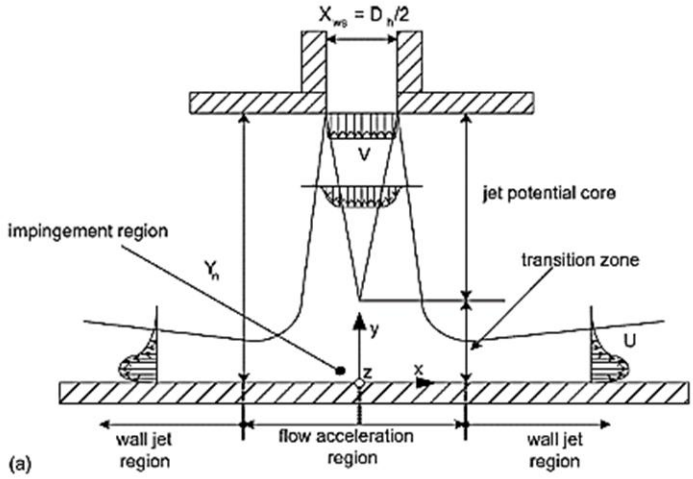

Figure 2: Flow characteristics of single jet impingement on flat surface [3]

The velocity profiles in an impinging jet are not only governed by the jet exit Reynolds number and nozzle geometry but also the distance of the target surface from the jet. In case of vertical impinging jets, at some distance upstream of the target surface the vertical velocity of the jet decreases rapidly and is gradually transformed into a horizontal component [5]. This region is often referred to as the stagnation region of the jet [7]. Giralt et al. [8] characterized the length of this region to be about 1.2 times the nozzle diameter from the stagnation point. At the stagnation point the velocity of the jet is zero while the static pressure is highest. The region of the flow beyond the stagnation point is called the wall jet region. In this region the flow accelerates as it moves some distance along the surface due to a favorable pressure gradient and the velocity profile is asymmetric as the flow is bounded by the target surface on one side and by the surrounding fluid on the other side as shown in Figure 2.

The main objective of this study is to examine the heat transfer of heat transfer of circular as well as square nozzles, arranged to form an in-line array. To achieve this goal, the characteristics of heat transfer over impinging plate will be studied therefore the local heat transfer will be estimated. This result carried out under different conditions such as, Reynolds number varied from 2000, 4000, 6000, 8000, and 10000. Four jets are array inline circular and square cross section. The spacing distance between jets are considered constant of (S/d = 6). The separation distance (H/d = 2, 4, 6, and 8).

2. Experimental Set-Up

The main parts of the experimental apparatus were a nozzle and an impingement surface, as shown in Figure 3. Air was supplied with an air compressor through a calibrated orifice flow meter. An air filter and a pressure

regulator are installed upstream of the orifice flow meter to filter the air and maintain the downstream pressure at 8 bar. The actual flow rate is controlled by a needle valve before the digital flow rate (SITRANS FUG1010– Simens Co., Germany). The nozzle is a pipe made from stainless steel with inner diameter of 9.53mm and length-to-diameter ratio of 76. This length ensures a fully developed flow over the Reynolds number range investigation. The nozzle is clamped on a carriage in an arrangement that allows its height above the impingement surface and its angle of impingement to be varied. The impinging plate (225mm * 425mm * 1.0mm thick stainless steel sheet) is clamped tightly and stretched between two copper bus bars. Approximately 8mm of the sheet on both sides are sandwiched in the bus bars to ensure firm grip. Because of the sheet thinness, lateral conduction is negligible and the surface provides constant heat flux situation, as reported by Attalla [19]. Figure 1b illustrates two directions that are commonly referred to as the uphill and downhill direction of the flow. The thermal images were obtained by an IR camera (model: IC120LV, TROTEC Co., EU) that was positioned under the heated plate opposite the impinging nozzle, as shown in Figure 1a. The infrared camera was used to measure local temperature from the uniform heat flux surface, which provides higher spatial resolution (384 * 288 pixels –accuracy ^28C, ^2%) of temperature than thermocouples. The TROTEC IC120VL infrared camera was used to record the local temperature distribution with a resolution of 0.25mm per pixel. One-dimensional energy balance across the heated plate shows a negligible temperature difference across it; therefore, the local temperature difference on the bottom surface is considered the same as that on the top side. The bottom side of heated plate was painted using a thin coat (model: ACRYLIC AG: 525, DongguantTianruiEle., China), which provides high emissivity.

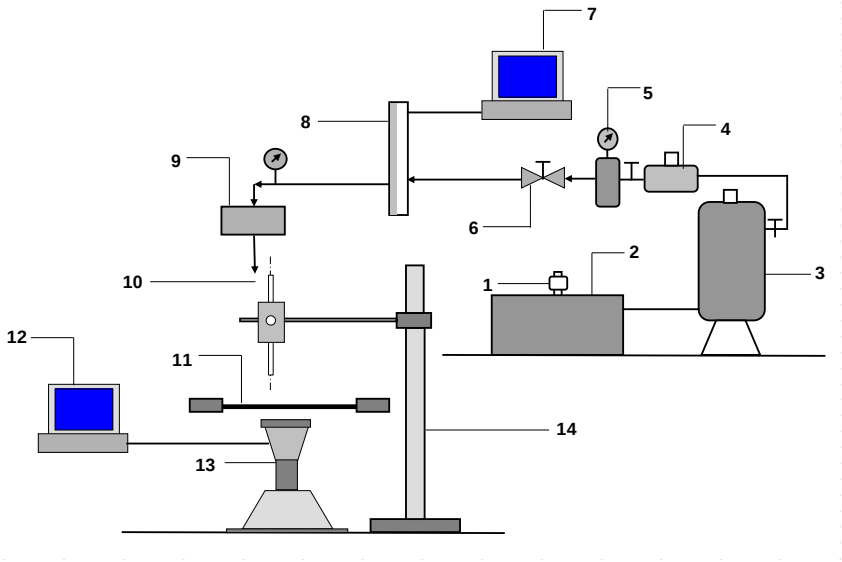

1—air filter, 2—air compressor, 3—air receiver, 4—air filter, 5—pressure regulator, 6—valve, 7—data acquisition unit, 8—digital flow meter, 9—plenum chamber, 10—circular nozzle, 11—target plate, 12—data acquisition unit, 13—infrared camera, 14—adjustable stand)

Figure 2: Experimental Set-Up

The impinging plate was heated using an AC power source through a voltage stabilizer. The voltage and current are measured by digital meter (model: M2332, LUCAS-NU¨ LLE, Germany), the ranges and accuracies of which are 400mV to 1000V ^ 0.5% and 40mA to 10A ^ 0.8%, respectively. The air jet temperature was measured by using a hot-wire thermo-anemometer (CFM-thermo-anemometer, model 407119A, EXTECH, USA) positioned at the outlet of the nozzle.

3. Data Reduction

The temperature distribution on the impinging plate is obtained by averaging three infrared thermal images for each inclined angle. The Nusselt number for the smooth surface is estimated using the following equation:

$$Nu = \frac{h.d}{k} \quad (1)$$

where h is the heat transfer coefficient (W/m2.K), calculated by the following equation:

$$h = \frac{Q_{con}}{T_s - T_j} \quad (2)$$

where T_s and T_j are surface and jet temperatures, respectively.

The heat transfer rate between the impinging jet and target plate Q_{conv} is estimated as:

$$Q_{Con} = Q_{ele} - Q_{loss} \quad (3)$$

Where

$$Q_{loss} = Q_{ra} + Q_{lonatss} \quad (4)$$

$$Q_{ele} = VI \quad (5)$$

$$Q_{rad} = \varepsilon\sigma(T_s^4 - T_\infty^4) \quad (6)$$

4. Results and Discussion

4.1 Temperature Contours

The surface temperature field of the one-jet without chevron nozzle for maximum Reynolds number (Re = 8000) and spacing distance 1 ≤ H/d ≤ 8 is shown in Figure 3. It is observed that the temperature field is clearly symmetric for all adjacent jets. Consequently, in the present study, the effect of the second stagnation point Nusselt number, on the center jet can be calculated from any neighbor jet.

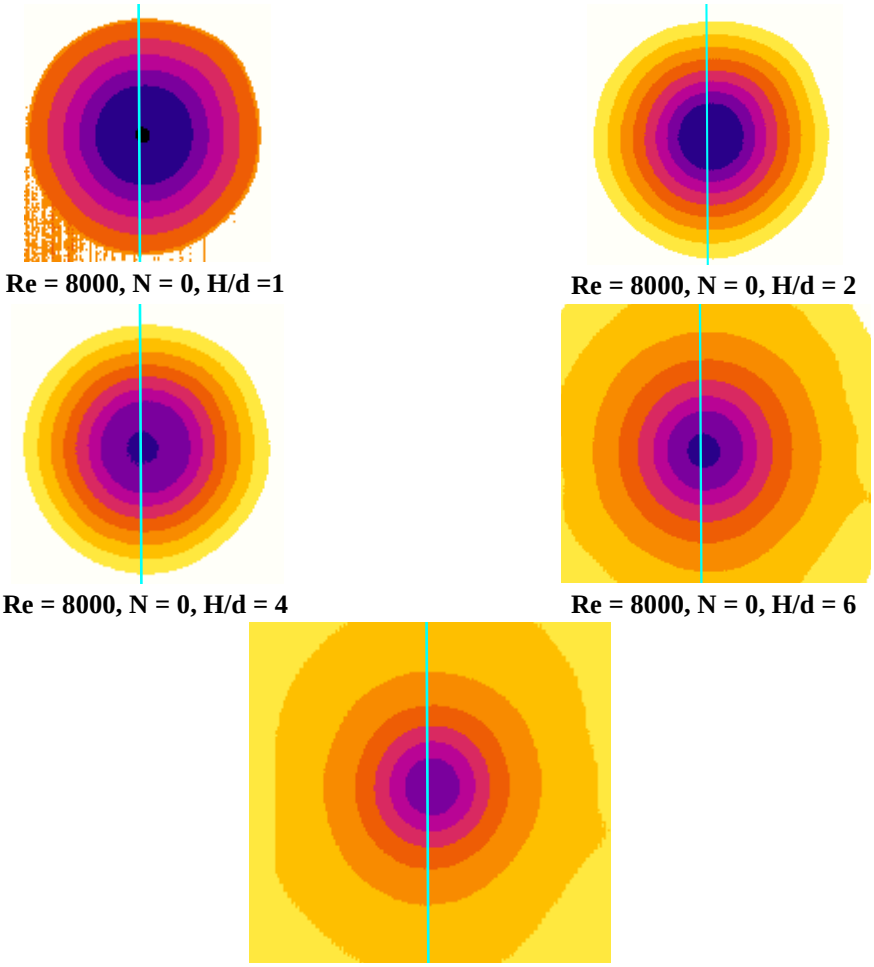

Re = 8000, N = 0, H/d =1 **Re = 8000, N = 0, H/d = 2**

Re = 8000, N = 0, H/d = 4 **Re = 8000, N = 0, H/d = 6**

Re = 8000, N = 0, H/d = 8

Figure 3: Temperature contours

4.3 Local Nusslet Number

The experimental results will focus firstly on the local heat transfer of a single nozzle. These results were measured with one jet of inner diameter of 10 mm and in the range of Reynolds number from 1500 to 8000. In addition, the separation distance H/d was chosen in the range from 1 to 8. Fig. 4 A to Fig. 4 E depicts the radial

distributions of the local Nusselt number for two Reynolds numbers (Re = 1500 and 8000) for example. The parameter is the separation distance ($1 \leq H/d \leq 8$). For the high Reynolds number (Re = 8000) and the low separation distance ($H/d \leq 2$), the impingement plate is within the potential core length of the free jet region. Thus, the heat transfer characteristics are very complicated due to the complex interaction between the impinging jet and the impingement plate [2, 3, 14-19] As shown in this figure, the local Nusselt number decreases rapidly from the stagnation point to a minimum value at X/d = 1.2 and then increases, giving the peak value at X/d = 2. Moving outward from the peak value, the heat transfer rate decreases monotonically. Similar profiles with the positions X/d = 1.2 and X/d = 2 for the minimum and maximum peak, respectively, were reported by other authors [19]. For the case of the separation distances (H/d = 4) a minimum and maximum does not occur any more. At the two positions of peak only the gradient changes. At high separation distances (H/d = 6) the local Nusselt number decreases monotonically upon going outward along the impingement plate and do ot show the peak value. For jet at plate separation distance larger than H/d = 6, the turbulence intensity of the impinging free jet zone has a maximum heat transfer at the stagnation point.

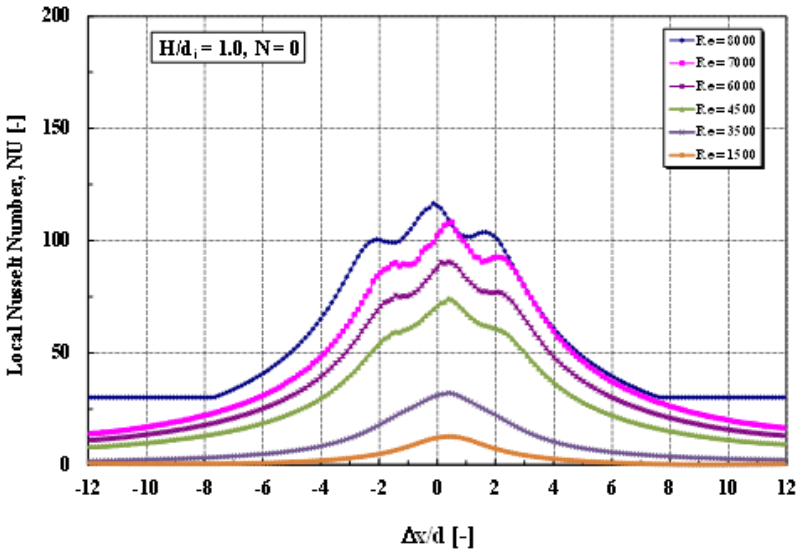

(A)

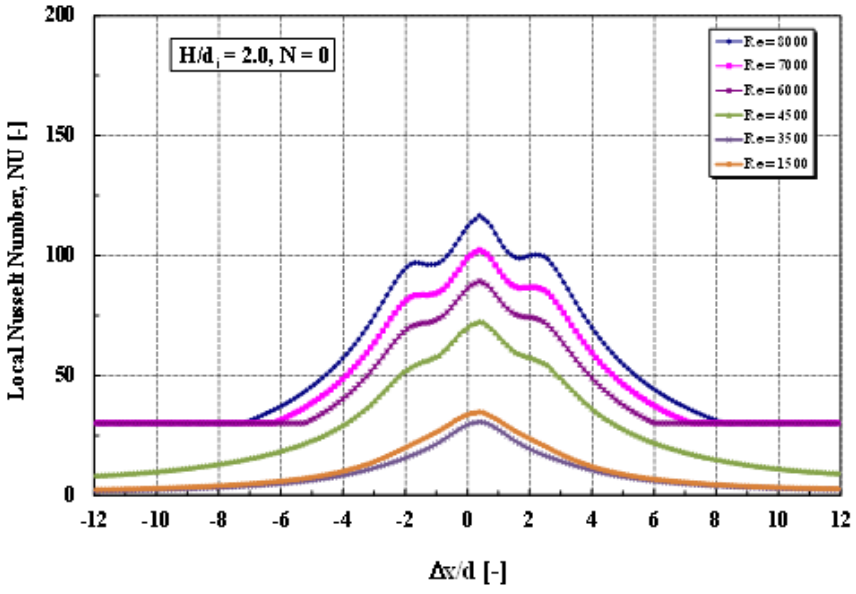

(B)

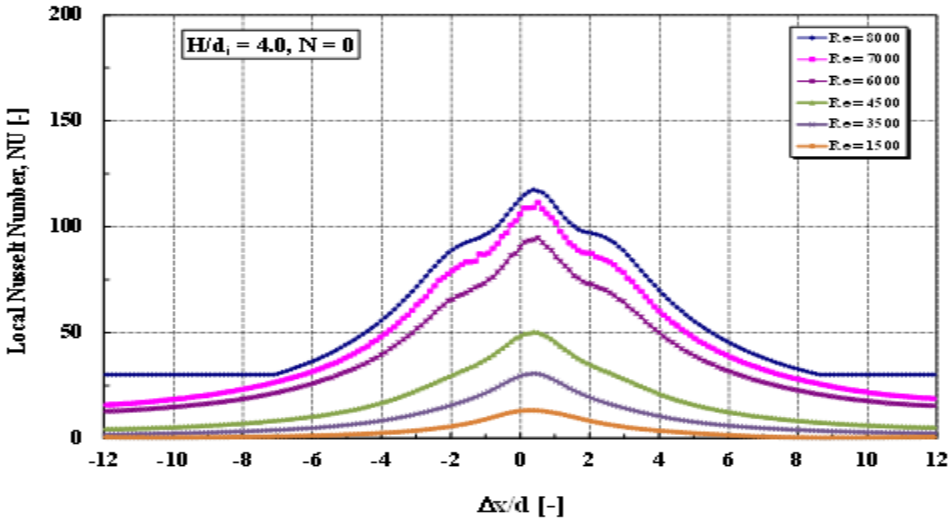

(C)

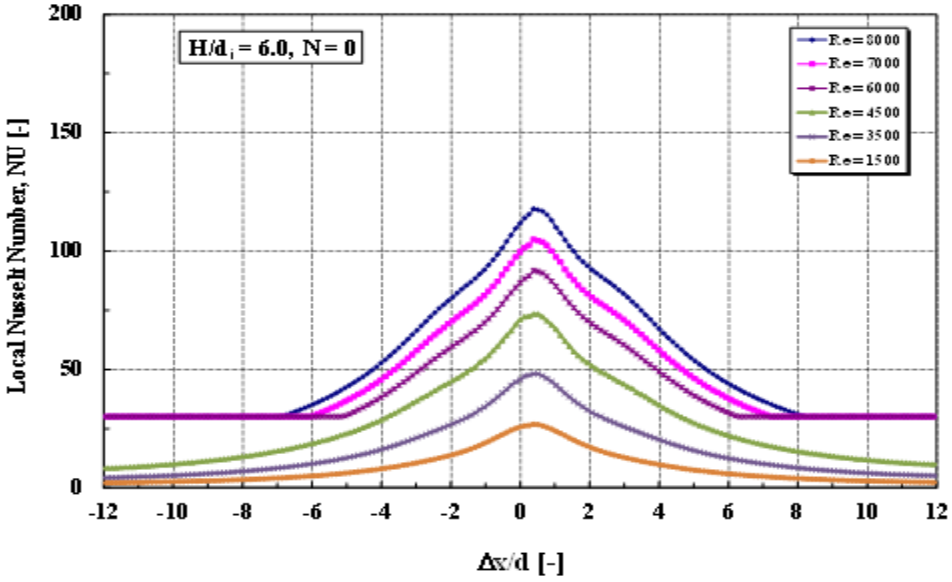

(D)

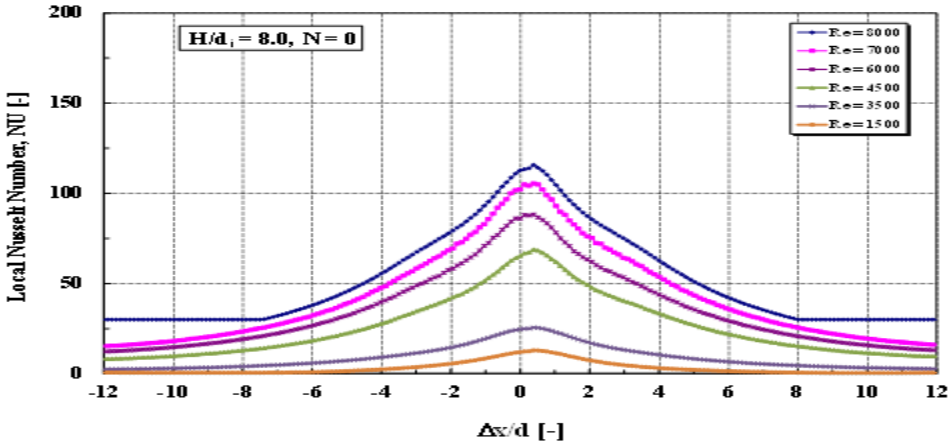

(E)

Figure 4: Variation of Local Nusselt number with Radial Distances (Δx/d) at Different Separation Distances 1 ≤ H/d ≤ 8

5. Conclusions

The effect of number of chevron nozzle on local and average Nusselt number for impinging plate is investigated experimentally. The number of chevron is varied from 0, 4, and 6. The separation distance H/d = 2, 4, 6, and 8). The Reynolds number is ranged from 8000 to 1400. The main conclusion from this study can be summarized as flow:

1. The local Nusselt number increases with increase of Reynolds number.
2. The local Nusselt number decreases with increase of chevron number for all Reynolds number.

References

[1]. Amini, Y. et al. (2015) 'Heat transfer of swirling impinging jets ejected from Nozzles with twisted tapes utilizing CFD technique', Case Studies in Thermal Engineering. doi: 10.1016/j.csite.2015.08.001.

[2]. Attalla, M. (2014) 'Stagnation Region Heat Transfer for Circular Jets Impinging on a Flat Plate', Experimental Heat Transfer, 28(2), pp. 139–155. doi: 10.1080/08916152.2013.829134.

[3]. Attalla, M. and Salem, M. (2013) 'Effect of nozzle geometry on heat transfer characteristics from a single circular air jet', Applied Thermal Engineering, 51(1–2), pp. 723–733.doi: 10.1016/j.applthermaleng.2012.09.032.

[4]. Bergman, T. L. et al. (2011) Fundamentals of Heat and Mass Transfer, Aerospace Engineering.

[5]. Gao, L. and Tong, S. J. (1998) Effect of jet hole arrays arrangement on impingement heat transfer.

[6]. Jeng, T. M., Tzeng, S. C. and Xu, R. (2014) 'Heat transfer characteristics of a rotating cylinder with a lateral air impinging jet', International Journal of Heat and Mass Transfer. doi: 10.1016/j.ijheatmasstransfer.2013.10.069.

[7]. Miyazaki, H. and Silberman, E. (1972) 'Flow and heat transfer on a flat plate normal to a two-dimensional laminar jet issuing from a nozzle of finite height', International Journal of Heat and Mass Transfer. doi: 10.1016/0017-9310(72)90034-8.

[8]. Rasool, A. A. A. and Hamad, F. A. (2013) 'Flow structure and cooling behavior of air impingement on a target plate', Central European Journal of Engineering, 3(0), pp. 400–409. doi: 10.2478/s13531-013-0103-z.

[9]. Reodikar, S. A., Chand, H. and Prabhu, S. V (2016) 'International Journal of Thermal Sciences In fluence of the ori fi ce shape on the local heat transfer distribution and axis switching by compressible jets impinging on fl at surface', 104, pp. 208–224. doi: 10.1016/j.ijthermalsci.2016.01.013.

[10]. San, J. Y. and Chen, J. J. (2014) 'Effects of jet-to-jet spacing and jet height on heat transfer characteristics of an impinging jet array', International Journal of Heat and Mass Transfer, 71, pp. 8–17. doi: 10.1016/j.ijheatmasstransfer.2013.11.079.

[11]. Singh, D., Premachandran, B. and Kohli, S. (2015) 'Effect of nozzle shape on jet impingement heat transfer from a circular cylinder', International Journal of Thermal Sciences. doi: 10.1016/j.ijthermalsci.2015.04.011.

[12]. Singh, H. and S. C. (2018) 'CFD Analysis of Effect of Reynolds Number on Local Heat Transfer Distribution for Jet Impingement on Smooth Plate by Incompressible Chevron Jet', International Journal of Engineering Technology Science and Research, 5(3), p. 6. Available at: www.ijetsr.com.

[13]. Transfer, H. and Insert, T. T. (2011) 'Heat Transfer and Friction Factor in a Tube Equipped with U-cut Twisted Tape Insert', Jordan Journal of Mechanical and Industrial Engineering, 5(6), pp. 559–565.

[14]. Trinh, X. T., Fénot, M. and Dorignac, E. (2016) 'The effect of nozzle geometry on local convective heat transfer to unconfined impinging air jets', Experimental Thermal and Fluid Science. doi: 10.1016/j.expthermflusci.2015.08.006.

[15]. Vinze, R. et al. (2016) 'Effect of compressibility and nozzle configuration on heat transfer by impinging air jet over a smooth plate', Applied Thermal Engineering. doi: 10.1016/j.applthermaleng.2016.02.069.

[16]. Viskanta, R. (1993) 'Nusselt-Reynolds Prize Paper Heat Transfer to Impinging Isothermal Gas and Flame Jets', Experimental Thermal and Fluid Scienc, 6, pp. 111–134.

[17]. Yang, G., Choi, M. and Lee, J. S. (1999) 'An experimental study of slot jet impingement cooling on concave surface: Effects of nozzle configuration and curvature', International Journal of Heat and Mass Transfer. doi: 10.1016/S0017-9310(98)00337-8.

[18]. Yang, H. Q., Kim, T. B. and Lu, T. J. (2011) 'Characteristics of annular impinging jets with/without swirling flow by short guide vanes', Science China Technological Sciences, 54(3), pp. 749–757. doi: 10.1007/s11431-010-4233-8.

[19]. Yangki Jung, B.E., M. S. (2004) Computer modeling of heat transfer of a mems based on micro-jet array air.